

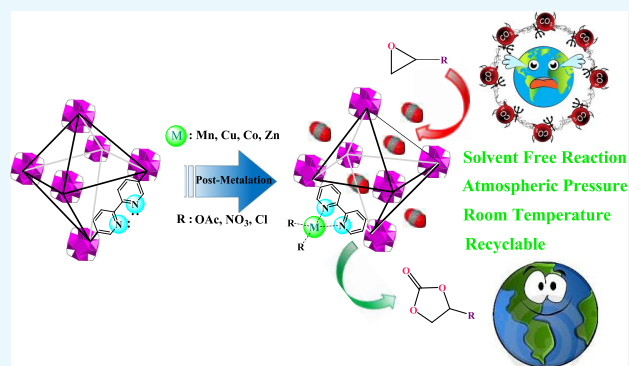
Diversity-Oriented Metal Decoration on UiO-Type Metal–Organic Frameworks: an Efficient Approach to Increase CO₂ Uptake and Catalytic Conversion to Cyclic Carbonates

Fataneh Norouzi and Hamid Reza Khavasi*[✉]

Department of Inorganic Chemistry and Catalysis, Shahid Beheshti University, General Campus, Evin, Tehran 1983963113, Iran

Supporting Information

ABSTRACT: A library of metallo-bipyridine UiO-type metal–organic frameworks (MOFs) has been successfully synthesized by postmetallation of a wide range of metal complexes into bidentate bipyridine moieties. Then, a systematic investigation is devoted to a catalytic evaluation of the resultant MOFs containing a binary Lewis acid function for the synthesis of cyclic carbonates from epoxides and carbon dioxide (CO₂). The result indicated that the metal-grafted MOFs exhibit improvement in terms of CO₂ uptake capacity and catalytic activity in comparison with their nonmetallated counterparts. The comprehensive investigation provides a valuable insight into the synergetic effects of MOF functionalities including metal node, grafted metal, and its counterion in the cycloaddition reaction. Furthermore, the metal coordination modulation due to its benefits such as being a solvent-free process, nearly full conversion to cyclic carbonates, high selectivity and high CO₂ uptake, applying atmospheric CO₂ pressure, and excellent stability and easy recyclability of the catalyst demonstrates them as promising candidates for practical utilization of CO₂ conversion into value-added chemicals.



INTRODUCTION

The growing CO₂ level as a result of anthropogenic activities has triggered global warming and climate change. On the other hand, CO₂ represents itself as an abundant and cheap source of C1 building block for producing numerous fine chemicals such as formic acid, carbon monoxide, cyclic carbonates, and others.^{1–4} Therefore, on the way toward a low carbon society and exploitation of a renewable carbon economy, selective adsorption of CO₂ and its subsequent chemical transformations are areas of intense current interest.^{5–10} In this sense, the synthesis of cyclic carbonate from CO₂ and epoxide considered the most effective utilization of CO₂ featuring a highly atom-economical reaction with minimal byproducts.^{11–18} Thus far, different types of catalysts developed for chemical CO₂ fixation with epoxides, including homogeneous and heterogeneous catalysts.^{19–25} Heterogeneous catalysts are superior to homogeneous catalysts in terms of product purification and the catalytic recovery process.^{26,27} Among them, metal–organic frameworks (MOFs) are recognized as promising tools in the field of CO₂ conversion.^{28,29} MOFs are porous materials constructed from organic struts linked by metal nodes.³⁰ Compared to traditional porous compounds, the modular nature of MOF functionalities driven from a rational combination of organic ligands and metal nodes endows tunable catalytic performance, adjustable porosity, and desirable topology.^{31,32} However, most of the CO₂ transformations under utility of MOFs suffer from all or at least one

either of limitations such as long reaction time, solvent assistant, high CO₂ pressure, and harsh reaction conditions, thus requiring high energy and capital costs. Thus, to circumvent the drawbacks, there is still a strong need for the de novo design of more efficient MOFs.^{33–37} Generally, MOFs take advantage of Lewis/Bronsted acid activation modes of metal nodes. Nevertheless, some modulations are invented to improve the CO₂ capture and conversion by incorporation of either open metal sites (Lewis acid) or N-donors (Lewis base) to activate epoxide and CO₂, respectively (Figure 1).^{38–41} Postmetallation of organic linkers with transition metals is emerging as an enabling trick to tune the catalytic properties of MOFs.^{38–40} As a result, the grafted metal ion serves as an additional Lewis acid center that profoundly affects the chemical, electrochemical, and porous capacity of the whole MOF system. From a mechanistic point of view, the initial step in MOF catalysis of CO₂ transformation into cyclic carbonate involves epoxide activation by an acid catalyst.^{38–42} Additionally, computational coupled with an experimental study by Morris and co-workers revealed that the open metal center in the metallo ligand acts as the primary Lewis acid site to facilitate CO₂ conversion.^{38,40} Hence, as the acidic function can be supplied from both metal nodes and metallo ligand

Received: July 3, 2019

Accepted: October 23, 2019

Published: November 6, 2019

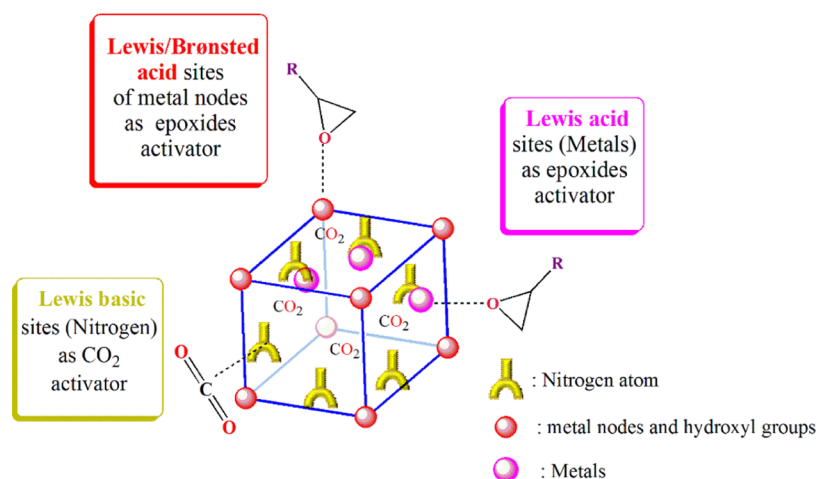


Figure 1. Presentation of MOF activation modes for epoxides and CO₂.

Scheme 1. Synthetic Procedure of Hf/Zr-Bipy-UiO-67 and Postmetallation Process for High CO₂ Capture and Conversion

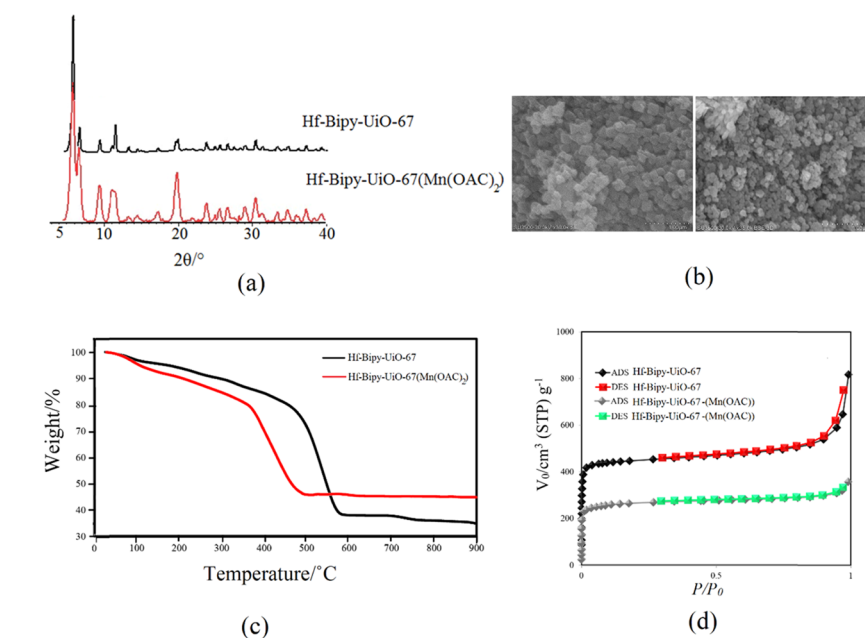
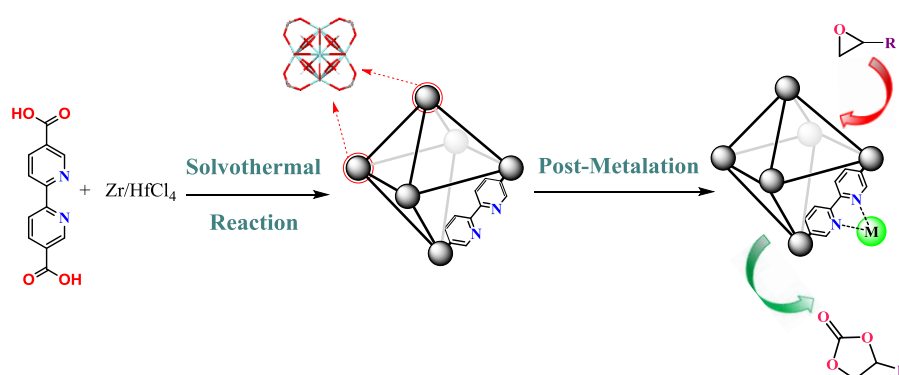


Figure 2. (a) PXRD patterns of Hf-Bipy-UiO-67 and Hf-Bipy-UiO-67(Mn(OAc)₂). (b) Scanning electron microscopy (SEM) images of Hf-Bipy-UiO-67 and Hf-Bipy-UiO-67(Mn(OAc)₂). (c) Thermogravimetric analysis (TGA) profiles of Hf-Bipy-UiO-67 and Hf-Bipy-UiO-67(Mn(OAc)₂). (d) Adsorption and desorption isotherms of N₂ at 77 K for Hf-Bipy-UiO-67 and Hf-Bipy-UiO-67(Mn(OAc)₂).

linkers, it is conceivable that simultaneous presence of the dual Lewis acid function can further increase the efficiency of CO₂ conversion to cyclic carbonates. However, literature survey

reveals that there is a scarce of investigation in this regard. In 2017, Demir et al. concluded that postmetallation of UiO-type zirconium MOFs with vanadium leads to inferior CO₂

conversion to their nonmetallated counterparts.³⁹ The low efficiency of the modulated MOFs is attributed to the reduction of surface area and pore volume as a result of postmetallation. In comparison, Zhu et al. evidenced that grafting the secondary open metal site into cyclam-based zirconium MOFs (VPI-100) is efficient.^{38,40}

N-heterocyclic ligands due to the presence of Lewis basic sites in the pores and surface are able to coordinate, trap, and interact with hazardous gaseous metal ions and other chemicals.^{43–45} Bipyridines are bidentate nitrogen ligands with rich coordination chemistry. A combination of the versatility of this moiety with high porosity and stability of MOFs leads to efficient systems, namely Bipy-UiO-67.

In this context, we report a postmetallation strategy for the synthesis of a novel series of Hf/Zr-Bipy-UiO-67(ML₂) (M = Co²⁺, Cu²⁺, Mn²⁺, Zn²⁺, and L = OAc⁻, NO₃⁻, and Cl⁻) and its catalytic evaluation for the synthesis of cyclic carbonates from epoxide and CO₂ under mild conditions (Scheme 1). To the best of our knowledge, this is the first study that systematically investigates the synergy of the metal node/M/L on the catalytic activity of MOFs for CO₂ utilization. It is demonstrated that the judicious choice of the metal node/M/L composite not only enhanced CO₂ capacity uptake but also improves the catalytic activity.

RESULTS AND DISCUSSION

Characterization of Metal-Grafted Hf/Zr-Bipy-UiO-67

MOFs. As we mentioned earlier, a series of postmetallated Bipy-UiO-67 MOFs, including Hf-Bipy-UiO-67(Mn(OAc)₂), Hf-Bipy-UiO-67(Cu(OAc)₂), Hf-Bipy-UiO-67(Co(OAc)₂), Hf-Bipy-UiO-67(Zn(OAc)₂), Hf-Bipy-UiO-67(Mn(NO₃)₂), Hf-Bipy-UiO-67(Cu(NO₃)₂), Hf-Bipy-UiO-67(Co(NO₃)₂), Hf-Bipy-UiO-67(Zn(NO₃)₂), Hf-Bipy-UiO-67(MnCl₂), Hf-Bipy-UiO-67(CuCl₂), Hf-Bipy-UiO-67(CoCl₂), Hf-Bipy-UiO-67(ZnCl₂), Zr-Bipy-UiO-67(Mn(OAc)₂), Zr-Bipy-UiO-67(Cu(OAc)₂), Zr-Bipy-UiO-67(MnCl₂), and Zr-Bipy-UiO-67(CuCl₂), was prepared under solvothermal reactions. The phase purity of the resulting MOFs was confirmed by powder X-ray diffraction (PXRD) experiments. The PXRD patterns exhibited the isoreticular and crystalline nature of these MOFs. The full PXRD patterns of MOFs are given in the Supporting Information. During the evaluation of the catalytic performance of the metal-grafted UiO-67 MOFs in CO₂ fixation reactions, Hf-Bipy-UiO-67(Mn(OAc)₂) acts as the best catalyst. Thus, in the following, full characterization of Hf-Bipy-UiO-67(Mn(OAc)₂) is discussed in detail. The PXRD pattern of Hf-Bipy-UiO-67(Mn(OAc)₂) indicated that similar to pristine MOFs, the crystallinity was well retained after postmetallation (Figure 2a).

Scanning electron microscopy (SEM) demonstrated that the morphologies of Hf-Bipy-UiO-67 and Hf-Bipy-UiO-67(Mn(OAc)₂) are cubic and spherical nanoparticles, respectively (Figure 2b). To evaluate the thermal stability of these MOFs, thermogravimetric analysis (TGA) investigation was conducted in an air atmosphere (Figure 2c). The TGA curve of the MOFs showed that decomposition of Hf-Bipy-UiO-67 starts from up to 500 °C, while that of Hf-Bipy-UiO-67(Mn(OAc)₂) starts at near 400 °C. These data illustrate the excellent chemical and thermal stability of the best catalyst.

The permanent porosity parameter was tested by N₂ adsorption–desorption isotherms at 77 K (Figure 2d). Similar to Hf-Bipy-UiO-67, Hf-Bipy-UiO-67(Mn(OAc)₂) due to the observation of the type I isotherm was identified as a

microporous material. The N₂ adsorption amounts of Hf-Bipy-UiO-67(Mn(OAc)₂) at low relative pressure ($P/P_0 < 0.1$) and high relative pressure ($P/P_0 < 0.99$) were 255 and 358 cm³ g⁻¹, respectively. Brunauer–Emmett–Teller surface areas for Hf-Bipy-UiO-67 and Hf-Bipy-UiO-67(Mn(OAc)₂) were obtained as 1040 and 637.32 m² g⁻¹, respectively. Furthermore, the Langmuir surface areas for Hf-Bipy-UiO-67 and Hf-Bipy-UiO-67(Mn(OAc)₂) were calculated to be 1797.5 and 1098.98 m² g⁻¹, respectively. Additionally, to investigate the CO₂ uptake capacity, we performed CO₂ adsorption of Hf-Bipy-UiO-67 and Hf-Bipy-UiO-67(Mn(OAc)₂) at 298 K (Figure 3).

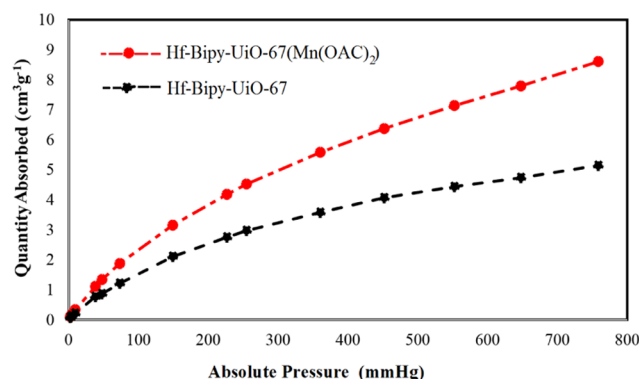
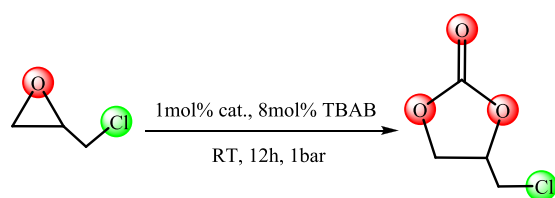


Figure 3. CO₂ adsorption isotherms of Hf-Bipy-UiO-67 and Hf-Bipy-UiO-67(Mn(OAc)₂) in 298 K.

As shown in Figure 2d, the CO₂ uptake value for Hf-Bipy-UiO-67(Mn(OAc)₂) at 800 mmHg pressure is 8.6 cm³ g⁻¹, while this value is dramatically decreased to 5.1 cm³ g⁻¹ for Hf-Bipy-UiO-67(Mn(OAc)₂).

The atomic ratio of manganese (Mn) in Hf-Bipy-UiO-67(Mn(OAc)₂) was analyzed by inductively coupled plasma-optical emission spectroscopy (ICP-OES). As expected, for each of the Hf atom in the UiO-67 cluster, there is one doped Mn atom, and thus, the ICP result exhibited an atomic ratio of 1:0.31 wt % (Hf/Mn).

Catalytic Cycloaddition of CO₂ and Epoxide. Due to the high density of the Lewis acid sites on the afforded MOFs and its capability of highly selective sorption of CO₂, we decided to evaluate the catalytic performance of the corresponding MOFs as bidentate Lewis acid catalysts to proceed the synthesis of cyclic carbonates from CO₂ and epoxides. The synthesis of 1,3-dioxolane-2-one from epichlorohydrin (ECH) was selected as a model reaction, and the results are summarized in Table 1. The solvent-free reactions were conducted at room temperature using CO₂ (1 bar), ECH (4.3 mmol), tetrabutylammonium bromide (TBAB) (8 mol %), and 1 mol % of various homogeneous and heterogeneous (MOF) catalysts for 12 h, and the resulting mixtures were analyzed by ¹H NMR to find the efficiency of the reactions based on conversion (see the Supporting Information). As seen in Table 1, employing heterogeneous Bipy-UiO-67 MOFs bearing Zr and Hf nodes led to good conversions (Table 1, entries 1 and 2). In comparison, screening the separate sections of these MOFs (homogeneous) including 2,2'-Bipy-5,5'-dicarboxylic acid (Bronsted acid/Lewis base), ZrCl₄ (Lewis acid), and HfCl₄ (Lewis acid) led to a dramatic decrease in conversion (Table 1, entries 3–5), demonstrating the versatility of the MOF system. Next, the effects of postmetallation on Zr- and Hf-based Bipy-UiO-67 MOFs were

Table 1. Catalytic Investigation of the Cycloaddition of CO₂ with Epichlorohydrin^a

entry	catalysts	conversion (%) ^b	TON	TOF (h ⁻¹)
1	Zr-Bipy-UiO-67	81 ± 1	81	6.71
2	Hf-Bipy-UiO-67	82 ± 2	83	6.83
3	2,2'-Bipy-5,5'-dicarboxylic acid	46 ± 2	46	3.85
4	ZrCl ₄	39 ± 3	39	3.26
5	HfCl ₄	38 ± 2	38	3.14
6	Zr-Bipy-UiO-67(MnCl ₂)	46 ± 3	46	3.81
7	Zr-Bipy-UiO-67(CuCl ₂)	44 ± 3	44	3.69
8	Hf-Bipy-UiO-67(MnCl ₂)	48 ± 2	48	3.98
9	Hf-Bipy-UiO-67(CuCl ₂)	49 ± 2	49	4.05
10	Hf-Bipy-UiO-67(CoCl ₂)	48 ± 1	48	4.02
11	Hf-Bipy-UiO-67(ZnCl ₂)	43 ± 4	43	3.57
12	Hf-Bipy-UiO-67(Mn(NO ₃) ₂)	66 ± 2	66	5.50
13	Hf-Bipy-UiO-67(Cu(NO ₃) ₂)	74 ± 2	74	6.17
14	Hf-Bipy-UiO-67(Co(NO ₃) ₂)	84 ± 1	84	7.01
15	Hf-Bipy-UiO-67(Zn(NO ₃) ₂)	86 ± 2	86	7.16
16	Zr-Bipy-UiO-67(Mn(OAc) ₂)	85 ± 1	85	7.08
17	Zr-Bipy-UiO-67(Cu(OAc) ₂)	52 ± 3	52	4.31
18	Hf-Bipy-UiO-67(Mn(OAc) ₂)	>99	99	8.25
19	Hf-Bipy-UiO-67(Cu(OAc) ₂)	85 ± 2	85	7.08
20	Hf-Bipy-UiO-67(Co(OAc) ₂)	74 ± 1	74	6.19
21	Hf-Bipy-UiO-67(Zn(OAc) ₂)	55 ± 3	55	4.62
22	Mn(OAc) ₂	43 ± 4	43	3.58

^aReaction conditions: epichlorohydrin (4.3 mmol), catalysts (1 mol % based on open metal sites; for entries 13 and 17, 1.2 mol %), n-Bu₄NBr (8 mol %), 1 bar CO₂, room temperature (ca. 29 °C), 12 h. All reactions were run at least three times, and the reported data are averages. ^bDetermined by liquid nuclear magnetic resonance (NMR) in CDCl₃.

investigated (Table 1, entries 6–21). Accordingly, Zr/Hf-Bipy-UiO-67 grafted by chlorine salts of Mn, Cu, Co, and Zn exhibited very poor catalytic performance (ranges of 43–49%) compared to the nongrafted counterparts (compare the conversions of entries 1 and 2 with 6–11). However, trying the reaction by replacing the nitrate salt of metals was shown to be effective as moderate to good conversions were obtained (Table 1, entries 12–15). Among them, using Hf-Bipy-UiO-67(Co(NO₃)₂) and Hf-Bipy-UiO-67(Zn(NO₃)₂) afforded superior results of 84 and 86% conversions, respectively (Table 1, entries 14 and 15). Next, observing the effects of metal counterions on this reaction, we further developed our study by evaluating the incorporation of acetate salt of the metals into Zr/Hf-Bipy-UiO-67 MOFs (Table 1, entries 16–21). As the result indicates, moderate to high conversion was achieved and Hf-Bipy-UiO-67(Mn(OAc)₂) with >99% conversion is recognized as the best catalyst for the synthesis of the desired cyclic carbonate (Table 1, entry 18). To gain knowledge on the efficiency of Hf-Bipy-UiO-67(Mn(OAc)₂), the reaction was carried out by using Mn(OAc)₂, in which the resulting conversion significantly decreased to 43% (Table 1, entry 22).

Careful looking of the overall results reveals that the kind of metal node and grafted metal complexes can greatly affect the catalytic activity of MOFs. Accordingly, Hf-based MOFs are more efficient than Zr-based MOFs in each of Cl, NO₃, and OAc reactionary collections. The more oxophilic nature of Hf relative to Zr could account for this observation.⁴⁶ Also, it is demonstrated that the catalytic conversions of MOFs that are grafted by M(NO₃)₂ and M(OAc)₂ are more than double that by M(Cl)₂. This phenomenon is attributed to the resonance characteristic in NO₃ and OAc ligands. As a result, the metal centers in these ligands feel more electron deficiency and tend to bind oxygen to nonelectron pairs of epoxides tightly.⁴⁷

After the demonstration of Hf-Bipy-UiO-67(Mn(OAc)₂) as the best catalyst, attention was paid to investigate the optimum set of the reaction conditions (Table 2). First, the amount of

Table 2. Effect of the Molar Ratio of the Hf-Bipy-UiO-67-(Mn(OAc)₂) Catalyst and TBAB on the ECH Synthesis^a

entry	catalyst (mol %) ^b	TBAB (mol %)	conversion (%) ^c
1	1	1	18 ± 1
2	1	2	38 ± 1
3	1	3	49 ± 2
4	1	4	57 ± 1
5	1	6	62 ± 3
6	1	8	>99
7	0.5	8	38 ± 2
8 ^d	1	8	>99
9	1	0	<1

^aReaction condition: ECH (4.3 mmol), 1 bar CO₂, room temperature, 12 h. All reactions were run at least three times, and the reported data are averages. ^bThe metal contents were determined by inductively coupled plasma-optical emission spectrometry (ICP-OES). ^cDetermined by liquid NMR in CDCl₃. ^d50 °C, 8 h.

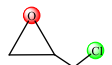
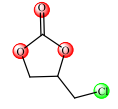
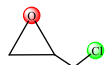
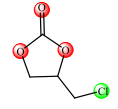
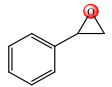
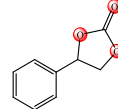
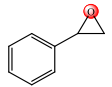
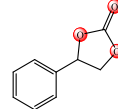
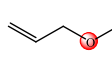
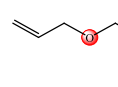
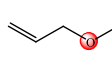
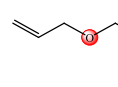
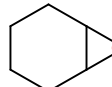
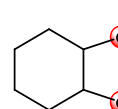
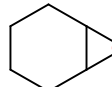
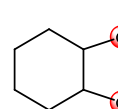
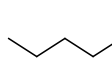
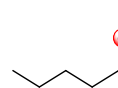
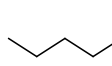
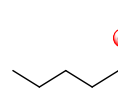
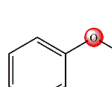
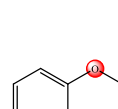
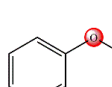
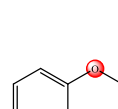
co-catalyst loading was evaluated, and it was found that a gradual increase in the loading amount of TBAB from 1 to 8% led to an increase in the conversion from 11 to 99% (Table 2, entries 1–6). Next, lowering the loading amount of the catalyst from 1 to 0.5% remarkably decreased the conversion to 38% (Table 2, entry 7). Therefore, it can be concluded that increasing the efficiency and amount of the catalyst is a directly proportional variation. In other words, increasing the concentration of the catalytic site improves the catalytic conversion. Also, it is realized that the presence of TBAB is critical for this transformation as the trace amount of the desired adduct was detected in the absence of the co-catalyst (Table 2, entry 9). Thus, it is disclosed that both the catalyst and TBAB have a dispensable role in this reaction. Running the reaction under heat conditions (50 °C) reduced the reaction time to 8 h without affecting the efficiency (Table 2, entry 8). However, for saving energy, the reaction was conducted at ambient temperature. Notably, for all of the reactions, no trace of the common byproducts such as 3-chloropropane-1,2-diol or polycarbonates was observed. Eventually, using 1 mol % Hf-Bipy-UiO-67(Mn(OAc)₂) and 8 mol % TBAB at room temperature for 12 h was established as the ideal condition (Table 2, entry 6).

Having identified the advantages of the catalytic activity of Hf-Bipy-UiO-67(Mn(OAc)₂), we assumed it worthwhile to compare the efficiency of Hf-Bipy-UiO-67(Mn(OAc)₂) to the earlier reported metal-immobilized MOFs in CO₂ fixation into ECH (Table 3). As summarized in Table 3, compared to

Table 3. Comparison of Reported Cycloaddition of CO₂ with ECH by Various Metal-Grafted MOF Catalysts

entry	catalysts	catalyst (mol %)	co-catalyst (mol %)	temperature (°C)	time (h)	pressure (bar)	conversion (%)	ref
1	MOF-53-VCl ₃	0.1	DMAP, 0.2	100	2	16	40	39
2	MOF-53-VCl ₄	0.1	DMAP, 0.2	100	2	16	50	39
3	VPI-100(Cu)	0.025	TBAB, 1	90	6	10	94	38
4	VPI-100(Ni)	0.025	TBAB, 1	90	6	10	96	38
5	Hf-VPI-100(Cu)	0.025	TBAB, 1	90	6	1.5	97	40
6	Hf-VPI-100(Ni)	0.025	TBAB, 1	90	6	1.5	89	40
7	Hf-Bipy-UiO-67-(Mn(OAc) ₂)	1	TBAB, 8	25	12	1	>99	this work

Table 4. Scope of the Cycloaddition Reaction of CO₂ with Epoxides^b

Entry	Epoxide	Cyclic Carbonates	Temperature (°C)	Time (h)	Conversion ^[a] (%)	TON	TOF (h ⁻¹)
1			25	12	< 99	99	8.25
2			50	8	< 99	99	12.35
3			25	12	20	20	1.66
4			50	4	< 99	99	24.75
5			25	12	31	31	2.58
6			50	4	< 99	99	24.75
7			25	12	38	38	3.16
8			50	4	< 99	99	24.75
9			25	12	21	21	1.75
10			50	4	95	95	23.75
11			25	12	17	17	1.41
12			50	4	< 99	99	24.75

^aDetermined by liquid NMR in CDCl₃. ^bReaction condition: Various epoxides (4.3 mmol), 1 bar CO₂.

MOF-53-VCl₃/VCl₄ as bipyridine UiO-type MOFs and metal-cyclam-based Zr/Hf MOFs denoted VPI-100, Hf-Bipy-UiO-67(Mn(OAc)₂) herein exhibits significant progress in terms of high conversion, mild reaction conditions, and low CO₂ pressure. Having obtained the optimal conditions (Table 2, entry 6), the combinatorial potential of the described procedure was investigated by using a range of epoxides (Table 4). In comparison to ECH, it can be seen that with an increase of the substituent bulk of epoxide substrates, the conversion of the desired cyclic carbonates dramatically decreased under room temperature conditions (Table 4, compare the conversion of entry 1 with entries 3, 5, 7, 9, and 11). This could be attributed to the steric effect of pores in

Hf-Bipy-UiO-67(Mn(OAc)₂) with large-size epoxides, which affects the diffusion rate of substrates and results in a decrease of conversion. To prove this claim, a control experiment was set for conversion of styrene oxide using HfCl₄/TBAB as the homogeneous catalyst. According to our experiment, 34% conversion of styrene carbonate was achieved under the optimized conditions obtained for ECH (Supporting Information, Figure S44). This result evidenced that bulky epoxides are sensitive to the hindrance effect of pores and reactions are taking place inside the pores.

To circumvent the hurdle of efficiency for bulkier epoxides, and knowing that the catalytic activity of Bipy-UiO-67(Mn(OAc)₂) is compatible under heat conditions (Table 2, entry

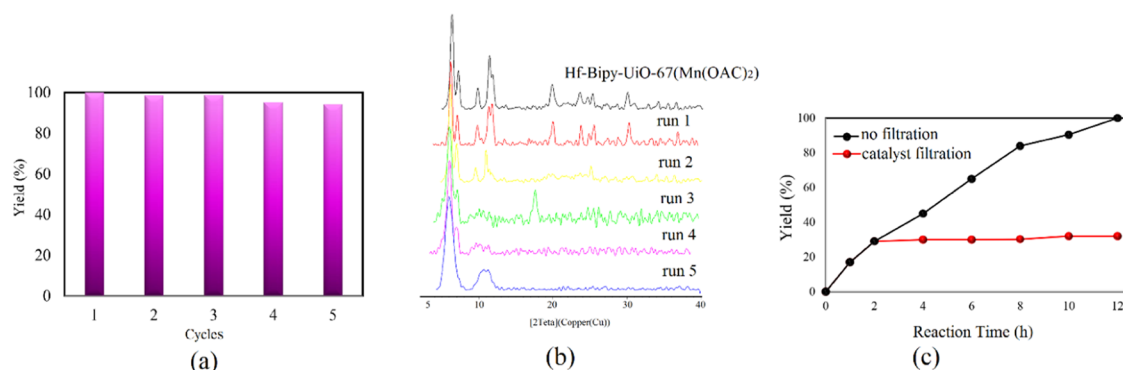


Figure 4. (a) Recycle experiments of Hf-Bipy-UiO-67(Mn(OAc)₂) for cycloaddition of CO₂ with ECH under solvent-free, 12 h, 1 bar, and room temperature conditions. Conversion for each cycle in percent: run 1, 99%; run 2, 98%; run 3, 98%; run 4, 96%; and run 5, 95%. (b) PXRD patterns of Hf-Bipy-UiO-67(Mn(OAc)₂) after each catalytic cycle and (c) leaching test of Hf-Bipy-UiO-67(Mn(OAc)₂).

8), the reactions of the bulky epoxides were carried out at 50 °C. Gratefully, except 2-butyloxirane with 95% conversion (Table 4, entry 10), all of the applied epoxides afforded the desired cyclic carbonates in nearly full conversion (Table 4, entries 4, 6, 8, 10, and 12).

To investigate the heterogeneity and stability of Hf-Bipy-UiO-67(Mn(OAc)₂), leaching and recyclability tests in the reaction of ECH and CO₂ were performed. As shown in Figure 4a, no significant decrease was observed in the conversion of the reaction after five cycles. Due to its high chemical stability, the recovered catalyst maintained the entirety of the MOF and crystallinity after each cycle as indicated by PXRD (Figure 4b). By filtration of the catalyst from the batch after 2 h, no catalytic activity was observed, which means that no leaching of catalytically active sites occurred (Figure 4c).

CONCLUSIONS

In summary, a series of metallo-bipyridine UiO-type MOFs based on Zr and Hf metal clusters was synthesized by a postmetallation approach. A comprehensive investigation of the effect of embedded metals (Mn²⁺, Cu²⁺, Co²⁺, and Zn²⁺) and counterions (OAc⁻, NO₃⁻, and Cl⁻) on the catalytic activities of the resulting MOFs was performed. The result revealed that the combination of catalytically active open metal sites, counterions, and unsaturated metal nodes significantly enhances the catalytic performance of the cycloaddition reaction. Additionally, the kind of counterion is an effective factor for the catalytic function of embedded metals as Lewis acid sites. Significantly, the result clearly showed that bulky epoxides are so sensitive to the hindrance effect of pores, and thus, the reaction is taking place inside the pores. Due to their outstanding chemical and thermal stability, these MOFs are good candidates for the catalytic reaction of CO₂ conversion under mild conditions.

EXPERIMENTAL SECTION

General. The organic ligand 2,2'-bipyridine-5,5'-dicarboxylic acid (BipyDC) and the metal salts were purchased and used without further purification from commercial suppliers (Sigma-Aldrich, Alfa Aesar, TCI, and others). Fourier transform infrared (FT-IR) spectra (4000–400 cm⁻¹) were collected in the solid state on a BOMEM-MB102 spectrometer using potassium bromide pellets. Powder X-ray diffraction (PXRD) experiments were performed on a Stöe StadiVari θ/θ powder X-ray diffractometer equipped with a graphite monochromator and Cu K α at 50 kV and 50 mA.

Thermogravimetric analysis (TGA) was carried out under continuous air flow and recorded on an SDT Q600 V20.9 Build 20 thermogravimetric analyzer with a heating rate of 20 °C per min (25–900 °C). NMR spectra were recorded on a Bruker DPX-300 spectrometer at 300 MHz for ¹H NMR and data for ¹H NMR are collected in CDCl₃ as follows: chemical shift (ppm), multiplicity (s, singlet; d, doublet; t, triplet; q, quarter; m, multiplet), coupling constant (Hz), and integration referenced to the appropriate solvent peak or 0 ppm for TMS. The dinitrogen (N₂) adsorption isotherm was measured at 77 K using a liquid-N₂ bath. The CO₂ adsorption isotherm was carried out at 298 K using a water bath. SEM images were taken on Hitachi SU 3500. Inductively coupled plasma-optical emission spectroscopy (ICP-OES 730-ES, Varian) was used for determination of the atomic ratio of Hf and Mn. Zr/Hf-Bipy-UiO-67 MOFs were prepared following the reported procedures.^{48,49}

Synthesis of Hf-Bipy-UiO-67. 2,2'-Bipyridine-5,5'-dicarboxylic acid (0.105 mmol, 0.25 g), HfCl₄ (0.105 mmol, 0.33 g), dimethylformamide (DMF) (4 mL), and acetic acid (AcOH) (200 μ L) were sealed in a glass vial. Then, the resulting mixture was initially sonicated for 10 min and subsequently heated at 120 °C for 24 h. After completion of the reaction, the mixture was cooled at room temperature. Then, the crystalline material was washed three times with DMF and MeOH. Finally, the resulting powder was centrifuged and activated under a vacuum oven at 90 °C overnight. Elemental analysis for Hf-Bipy-UiO-67, calcd: C 32.55%, H 1.50%, N 6.33%, found: C 32.01%, H 1.42%, N 6.10%. FT-IR (4000–400 cm⁻¹): 1596.94 (br), 1427.22 (br), 10164.92 (w), 1026.06 (w), 856.33 (w), 779.18 (m), 663.46 (s), 439.74 (m), 416.59 (w).

Synthesis of Zr-Bipy-UiO-67. 2,2'-Bipyridine-5,5'-dicarboxylic acid (0.105 mmol, 0.25 g), ZrCl₄ (0.105 mmol, 0.24 g), DMF (4 mL), and AcOH (200 μ L) were sealed in a glass vial. Then, the resulting mixture was initially sonicated for 10 min and subsequently heated at 120 °C for 24 h. After completion of the reaction, the mixture was cooled at room temperature. Then, the crystalline material was washed three times with DMF and MeOH. Finally, the resulting powder was centrifuged and activated under a vacuum oven at 90 °C overnight. Elemental analysis for Zr-Bipy-UiO-67, calcd: C 40.55%, H 1.87%, N 7.88%, found: C 40.8%, H 1.75%, N 7.98%. FT-IR (4000–400 cm⁻¹): 1689.52 (br), 1596.94 (br), 1419.50 (s), 1311.50 (m), 1249.78 (w), 1126.06 (m), 1026.06 (m), 984.91 (w), 779.18 (s), 655.75 (s), 426.88 (m).

Postmetallation of Hf/Zr-Bipy-UiO-67. All of the metal-grafted MOFs were prepared as follows: The dehydrated metal salts (0.25 mmol, 5 equiv) were dissolved in 10 mL of acetonitrile (MeCN) and then Hf/Zr-Bipy-UiO-67 (0.05 mmol, 1 equiv) was added to the solution. Subsequently, the mixtures were sonicated (20 min) and heated at 60 °C for 24 h. After completion of the reaction, the mixtures were cooled at room temperature and the resulting crystalline powders were washed three times with MeCN and MeOH. Finally, the afforded MOFs were activated under a vacuum oven at 90 °C overnight. The metal contents were determined by inductively coupled plasma-optical emission spectrometry (ICP-OES), Spectro Arcos, Germany.

Hf-Bipy-UiO-67(MnCl₂). Elemental analysis for Hf-Bipy-UiO-67(MnCl₂), calcd: C 27.03%, H 1.25%, N 5.25%, found: C 27.80%, H 1.21%, N 5.14%. FT-IR (4000–400 cm⁻¹): 1704.95 (s), 1512.8 (s), 1396.36 (m), 1108.35 (m), 1002.91 (w), 771.47 (m), 655.75 (s), 439.75 (m), 416.59 (w).

Hf-Bipy-UiO-67(CoCl₂). Anal calcd: C 26.83%, H 1.24%, N 5.21%, found: C 25.93%, H 1.4%, N 5.29%. FT-IR (4000–400 cm⁻¹): 1620.09 (s), 1373.22 (s), 1164.92 (w), 1033.77 (m), 856.33 (w), 779.18 (m), 678.89 (s), 570.89 (w), 447.45 (w), 416.59 (w).

Hf-Bipy-UiO-67(CuCl₂). Anal calcd: C 26.60%, H 1.23%, N 5.17%, found: C 26.71%, H 1.45%, N 5.10%. FT-IR (4000–400 cm⁻¹): 1620.09 (s), 1396.33 (s), 1164.92 (w), 1041.48 (m), 856.33 (w), 779.18 (m), 671.18 (s), 455.17 (w), 424.31(w).

Hf-Bipy-UiO-67(ZnCl₂). Anal calcd: C 26.51%, H 1.22%, N 5.15%, found: C 26.10%, H 1.10%, N 5.22%. FT-IR (4000–400 cm⁻¹): 1604.66 (s), 1419.50 (s), 1164.92 (w), 1033.77 (m), 856.33 (w), 779.18 (m), 671.18 (s), 586.32 (w), 426.88 (w).

Zr-Bipy-UiO-67(MnCl₂). Anal calcd: C 32.33%, H 1.49%, N 6.28%, found: C 33.02%, H 1.53, N 6.12%. FT-IR (4000–400 cm⁻¹): 1612.37 (br), 1396.36 (s), 1249.78 (w), 1164.92 (m), 1033.77 (m), 856.33 (w), 771.74 (m), 648.03 (br), 563.17 (w), 426.28 (w).

Zr-Bipy-UiO-67(CuCl₂). Anal calcd: C 31.71%, H 1.46%, N 6.16%, found: C 31.32%, H 1.21%, N 6.00%. FT-IR (4000–400 cm⁻¹): 1612.37 (br), 1419.50 (s), 1126.35 (w), 1041.48 (m), 856.33 (w), 771.74 (m), 655.75 (br), 455.17 (w).

Hf-Bipy-UiO-67(Mn(OAc)₂). Anal calcd: C 38.97%, H 2.56%, N 5.68%, found: C 38.25%, H 2.67%, N 5.33%. FT-IR (4000–400 cm⁻¹): 1604.66 (br), 1411.79 (s), 1164.92 (w), 1026.06 (m), 846.62 (w), 779.18 (m), 655.75 (br), 439.74 (w).

Hf-Bipy-UiO-67(Co(OAc)₂). Anal calcd: C 38.66%, H 2.54%, N 5.63%, found: C 37.92%, H 2.27%, N 5.87%. FT-IR (4000–400 cm⁻¹): 1596.94 (br), 1419.50 (s), 1164.92 (w), 1026.06 (m), 848.62 (w), 779.18 (m), 671.18 (br), 486.03 (w), 424.31 (w).

Hf-Bipy-UiO-67(Cu(OAc)₂). Anal calcd: C 38.30%, H 2.52%, N 5.58%, found: C 38%, H 2.10%, N 5.12%. FT-IR (4000–400 cm⁻¹): 1620.09 (s), 1380.93 (s), 1164.92 (w), 1041.48 (m), 848.62 (w), 779.18 (m), 655.75 (br), 424.31 (w).

Hf-Bipy-UiO-67(Zn(OAc)₂). Anal calcd: C 38.15%, H 2.51%, N 5.56%, found: C 37.81%, H 2.10%, N 5.22%. FT-IR (4000–400 cm⁻¹): 1596.94 (s), 1419.50 (s), 1164.92 (w), 1026.06 (m), 848.62 (w), 856.33 (w), 779.18 (m), 663.46 (br), 532.31 (w), 462.88 (w), 424.31 (w).

Zr-Bipy-UiO-67(Mn(OAc)₂). Anal calcd: C 46.37%, H 3.12%, N 6.90%, found: C 45.92%, H 3.33%, N 6.13%. FT-IR (4000–

400 cm⁻¹): 1612.37 (s), 1380.93 (s), 1164.92 (w), 1033.77 (m), 846.62 (w), 779.18 (m), 648.03 (br), 462.88 (w), 424.31 (w).

Zr-Bipy-UiO-67(Cu(OAc)₂). Anal calcd: C 47.35%, H 3.05%, N 6.76%, found: C 48.20%, H 2.92%, N 6.32%. FT-IR (4000–400 cm⁻¹): 1620.09 (s), 1388.65 (s), 1141.78 (w), 1041.48 (m), 848.62 (w), 779.18 (m), 648.03 (m), 478.31 (m), 424.31 (w).

Hf-Bipy-UiO-67(Mn(NO₃)₂). Anal calcd: C 23.03%, H 1.06%, N 9.02%, found: C 23.11%, H 1.32%, N 8.72%. FT-IR (4000–400 cm⁻¹): 1604.66 (s), 1419.50 (s), 1164.92 (w), 1033.77 (m), 856.33 (w), 779.18 (m), 686.61 (br), 439.74 (s).

Hf-Bipy-UiO-67(Co(NO₃)₂). Anal calcd: C 23.03%, H 1.06%, N 8.95%, found: C 23.23%, H 1.12%, N 8.23%. FT-IR (4000–400 cm⁻¹): 1604.66 (s), 1419.50 (s), 1164.92 (w), 1026.06 (w), 864.05 (w), 779.18 (m), 671.18 (br), 547.74 (w), 455.17 (w), 424.31 (w).

Hf-Bipy-UiO-67(Cu(NO₃)₂). Anal calcd: C 22.86%, H 1.05%, N 8.89%, found: C 22.30%, H 1.43%, N 8.53%. FT-IR (4000–400 cm⁻¹): 1596.94 (s), 1419.50 (s), 1164.92 (m), 1026.06 (m), 856.33 (w), 771.47 (m), 663.46 (br), 570.89 (w), 447.45 (w).

Hf-Bipy-UiO-67(Zn(NO₃)₂). Anal calcd: C 22.80%, H 1.05%, N 8.86%, found: C 21.93%, H 1.03, N 8.49%. FT-IR (4000–400 cm⁻¹): 1620.09 (br), 1427.22 (s), 1164.92 (w), 1041.48 (w), 840.90 (w), 779.18 (m), 671.18 (m), 578.60 (w), 470.60 (w).

General Procedure for the Catalytic Cycloaddition of Epoxides with CO₂. The reactions were conducted under solvent-free conditions in a glass reactor equipped with a magnetic stirrer. The corresponding epoxides (4.3 mmol), tetrabutylammonium bromide (TBAB) (8 mol %), and the catalysts (1 mol %, based on open metal sites) were added to a glass reactor under 1 bar pressure of CO₂ for the desired temperatures and times. After each catalytic reaction, the catalyst was separated by centrifugation, and the resulting product was analyzed by ¹H NMR. For examining the reusability of the MOFs, after centrifugation, the MOFs were washed with MeOH three times and subsequently activated under a vacuum oven at 90 °C overnight. The afforded MOFs were used for the second run of the reaction.

Leaching Test. After 2 h of the reaction, the catalyst was separated from the reactor by a syringe. Then, the reaction was continued under free-catalyst conditions for 9 h. The ¹H NMR results clearly demonstrated that the catalyst was completely heterogeneous and no further increase in the conversion of the reaction was observed.

■ ASSOCIATED CONTENT

Supporting Information

The Supporting Information is available free of charge on the ACS Publications website at DOI: [10.1021/acsomega.9b02035](https://doi.org/10.1021/acsomega.9b02035).

PXRD patterns of metal-grafted Bipy-UiO-67 MOFs; NMR spectrum for data reported in Tables 1, 2, and 4; NMR spectra of recyclability tests (Figures S1–S47) (PDF)

■ AUTHOR INFORMATION

Corresponding Author

*E-mail: h-khavasi@sbu.ac.ir, khavasihr@gmail.com. Tel: +98 21 29903105. Fax: +98 21 22431661.

ORCID 

Hamid Reza Khavasi: 0000-0003-2303-3668

Notes

The authors declare no competing financial interest.

ACKNOWLEDGMENTS

We would like to thank the Graduate Study Councils of Shahid Beheshti University, General Campus, for financial support.

REFERENCES

- (1) Arakawa, H.; Aresta, M.; Armor, J. N.; Barteau, M. A.; Beckman, E. J.; Bell, A. T.; Bercaw, J. E.; Creutz, C.; Dinjus, E.; Dixon, D. A.; Domen, K.; DuBois, D. L.; Eckert, J.; Fujita, E.; Gibson, D. H.; Goddard, W. A.; Goodman, D. W.; Keller, J.; Kubas, G. J.; Kung, H. H.; Lyons, J. E.; Manzer, L. E.; Marks, T. J.; Morokuma, K.; Nicholas, K. M.; Periana, R.; Que, L.; Rostrup-Nielsen, J.; Sachtler, W. M. H.; Schmidt, L. D.; Sen, A.; Somorjai, G. A.; Stair, P. C.; Stults, B. R.; Tumas, W. Catalysis Research of Relevance to Carbon Management: Progress, Challenges, and Opportunities. *Chem. Rev.* **2001**, *101*, 953–996.
- (2) Sakakura, T.; Choi, J.-C.; Yasuda, H. Transformation of Carbon Dioxide. *Chem. Rev.* **2007**, *107*, 2365–2387.
- (3) Liu, Q.; Wu, L.; Jackstell, R.; Beller, M. Using carbon dioxide as a building block in organic synthesis. *Nat. Commun.* **2015**, *6*, No. 5933.
- (4) Wang, X.; Zhou, Y.; Guo, Z.; Chen, G.; Li, J.; Shi, Y.; Liu, Y.; Wang, J. Heterogeneous conversion of CO₂ into cyclic carbonates at ambient pressure catalyzed by ionothermal-derived meso-macroporous hierarchical poly(ionic liquid)s. *Chem. Sci.* **2015**, *6*, 6916–6924.
- (5) Hu, Z.; Wang, Y.; Shah, B. B.; Zhao, D. CO₂ Capture in Metal–Organic Framework Adsorbents: An Engineering Perspective. *Adv. Sustainable Syst.* **2019**, *3*, No. 1800080.
- (6) Cao, X.; Wang, Z.; Qiao, Z.; Zhao, S.; Wang, J. Penetrated COF channels: amino environment and suitable size for CO₂ preferential adsorption and transport in mixed matrix membranes. *ACS Appl. Mater. Interfaces* **2019**, *11*, 5306–5313.
- (7) Yu, B.; He, L. N. Upgrading carbon dioxide by incorporation into heterocycles. *ChemSusChem* **2015**, *8*, 52–62.
- (8) Aresta, M.; Dibenedetto, A.; Angelini, A. Catalysis for the valorization of exhaust carbon: from CO₂ to chemicals, materials, and fuels. Technological use of CO₂. *Chem. Rev.* **2014**, *114*, 1709–1742.
- (9) Appel, A. M.; Bercaw, J. E.; Bocarsly, A. B.; Dobbek, H.; DuBois, D. L.; Dupuis, M.; Ferry, J. G.; Fujita, E.; Hille, R.; Kenis, P. J.; et al. Frontiers, opportunities, and challenges in biochemical and chemical catalysis of CO₂ fixation. *Chem. Rev.* **2013**, *113*, 6621–6658.
- (10) Cokoja, M.; Bruckmeier, C.; Rieger, B.; Herrmann, W. A.; Kühn, F. E. Umwandlung von Kohlendioxid mit Übergangsmetall-Homogenkatalysatoren: eine molekulare Lösung für ein globales Problem? *Angew. Chem.* **2011**, *123*, 8662–8690.
- (11) Li, J.-Y.; Han, L.-H.; Xu, Q.-C.; Song, Q.-W.; Liu, P.; Zhang, K. A Cascade Strategy for Atmospheric Pressure CO₂ Fixation to Cyclic Carbonates via Silver Sulfadiazine and Et₄NBr Synergistic Catalysis. *ACS Sustainable Chem. Eng.* **2019**, *7*, 3378–3388.
- (12) Wang, C.; Song, Q.-W.; Zhang, K.; Liu, P.; Wang, J.; Wang, J.; Zhang, H.; Wang, J. Atomic zinc dispersed on graphene synthesized for active CO₂ fixation to cyclic carbonates. *Chem. Commun.* **2019**, *55*, 1299–1302.
- (13) Kamphuis, A. J.; Picchioni, F.; Pescarmona, P. P. CO₂-fixation into cyclic and polymeric carbonates: principles and applications. *Green Chem.* **2019**, *21*, 406–448.
- (14) Paddock, R. L.; Nguyen, S. T. Chemical CO₂ fixation: Cr (III) salen complexes as highly efficient catalysts for the coupling of CO₂ and epoxides. *J. Am. Chem. Soc.* **2001**, *123*, 11498–11499.
- (15) North, M.; Pasquale, R. Mechanism of cyclic carbonate synthesis from epoxides and CO₂. *Angew. Chem.* **2009**, *121*, 2990–2992.
- (16) Yao, C.; Zhou, S.; Kang, X.; Zhao, Y.; Yan, R.; Zhang, Y.; Wen, L. A Cationic Zinc–Organic Framework with Lewis Acidic and Basic Bifunctional Sites as an Efficient Solvent-Free Catalyst: CO₂ Fixation and Knoevenagel Condensation Reaction. *Inorg. Chem.* **2018**, *57*, 11157–11164.
- (17) Bhanja, P.; Modak, A.; Bhaumik, A. Supported porous nanomaterials as efficient heterogeneous catalysts for CO₂ fixation reactions. *Chem. – Eur. J.* **2018**, *24*, 7278–7297.
- (18) Kumatabara, Y.; Okada, M.; Shirakawa, S. Triethylamine Hydroiodide as a Simple Yet Effective Bifunctional Catalyst for CO₂ Fixation Reactions with Epoxides under Mild Conditions. *ACS Sustainable Chem. Eng.* **2017**, *5*, 7295–7301.
- (19) Maeda, C.; Shimonishi, J.; Miyazaki, R.; Hasegawa, J.-y.; Ema, T. Highly active and robust metalloporphyrin catalysts for the synthesis of cyclic carbonates from a broad range of epoxides and carbon dioxide. *Chem. – Eur. J.* **2016**, *22*, 6556–6563.
- (20) Shaikh, R. R.; Pornpraprom, S.; D’Elia, V. Catalytic strategies for the cycloaddition of pure, diluted, and waste CO₂ to epoxides under ambient conditions. *ACS Catal.* **2018**, *8*, 419–450.
- (21) Liu, S.; Suematsu, N.; Maruoka, K.; Shirakawa, S. Design of bifunctional quaternary phosphonium salt catalysts for CO₂ fixation reaction with epoxides under mild conditions. *Green Chem.* **2016**, *18*, 4611–4615.
- (22) Beyzavi, M. H.; Stephenson, C. J.; Liu, Y.; Karagiari, O.; Hupp, J. T.; Farha, O. K. Metal–organic framework-based catalysts: chemical fixation of CO₂ with epoxides leading to cyclic organic carbonates. *Front. Energy Res.* **2015**, *2*, 63–73.
- (23) Liang, J.; Huang, Y.-B.; Cao, R. Metal–organic frameworks and porous organic polymers for sustainable fixation of carbon dioxide into cyclic carbonates. *Coord. Chem. Rev.* **2019**, *378*, 32–65.
- (24) Kurisingal, J. F.; Rachuri, Y.; Pillai, R. S.; Gu, Y.; Choe, Y.; Park, D.-W. Ionic liquid-functionalized UiO-66 framework: An experimental and theoretical study on the cycloaddition of CO₂ and epoxide. *ChemSusChem* **2019**, *12*, 1033–1042.
- (25) Patel, P.; Parmar, B.; Kureshy, R. I.; Khan, N.; Suresh, E. Efficient Solvent-Free Carbon Dioxide Fixation Reactions with Epoxides Under Mild Conditions by Mixed-Ligand Zinc (II) Metal–Organic Frameworks. *ChemCatChem* **2018**, *10*, 2401–2408.
- (26) Maya, E. M.; Verde-Sesto, E.; Mantione, D.; Iglesias, M.; Mecerreyes, D. New poly (ionic liquid) s based on poly (azomethine-pyridinium) salts and its use as heterogeneous catalysts for CO₂ conversion. *Eur. Polym. J.* **2019**, *110*, 107–113.
- (27) Xiao, L.-F.; Li, F.-W.; Peng, J.-J.; Xia, C.-G. Immobilized ionic liquid/zinc chloride: Heterogeneous catalyst for synthesis of cyclic carbonates from carbon dioxide and epoxides. *J. Mol. Catal. A: Chem.* **2006**, *253*, 265–269.
- (28) Choi, K. M.; Kim, D.; Rungtaweeworant, B.; Trickett, C. A.; Barmanbek, J. T. D.; Alshammari, A. S.; Yang, P.; Yaghi, O. M. Plasmon-enhanced photocatalytic CO₂ conversion within metal–organic frameworks under visible light. *J. Am. Chem. Soc.* **2017**, *139*, 356–362.
- (29) Li, P.-Z.; Wang, X.-J.; Liu, J.; Lim, J. S.; Zou, R.; Zhao, Y. A triazole-containing metal–organic framework as a highly effective and substrate size-dependent catalyst for CO₂ conversion. *J. Am. Chem. Soc.* **2016**, *138*, 2142–2145.
- (30) Li, H.; Eddaoudi, M.; O’Keeffe, M.; Yaghi, O. M. Design and synthesis of an exceptionally stable and highly porous metal-organic framework. *Nature* **1999**, *402*, 276.
- (31) Papaefstathiou, G. S.; MacGillivray, L. R. Inverted metal–organic frameworks: solid-state hosts with modular functionality. *Coord. Chem. Rev.* **2003**, *246*, 169–184.
- (32) Lee, J.; Farha, O. K.; Roberts, J.; Scheidt, K. A.; Nguyen, S. T.; Hupp, J. T. Metal–organic framework materials as catalysts. *Chem. Soc. Rev.* **2009**, *38*, 1450–1459.
- (33) Mottillo, C.; Friščić, T. Carbon dioxide sensitivity of zeolitic imidazolate frameworks. *Angew. Chem., Int. Ed.* **2014**, *53*, 7471–7474.
- (34) Zhang, W.; Hu, Y.; Ge, J.; Jiang, H.-L.; Yu, S.-H. A Facile and General Coating Approach to Moisture/Water-Resistant Metal–

Organic Frameworks with Intact Porosity. *J. Am. Chem. Soc.* **2014**, *136*, 16978–16981.

(35) Yao, J.; Wang, H. Zeolitic imidazolate framework composite membranes and thin films: synthesis and applications. *Chem. Soc. Rev.* **2014**, *43*, 4470–4493.

(36) Pera-Titus, M. Porous inorganic membranes for CO₂ capture: present and prospects. *Chem. Rev.* **2014**, *114*, 1413–1492.

(37) Zhang, M.; Chu, B.; Li, G.; Xiao, J.; Zhang, H.; Peng, Y.; Li, B.; Xie, P.; Fan, M.; Dong, L. Triethanolamine-modified mesoporous SBA-15: Facile one-pot synthesis and its catalytic application for cycloaddition of CO₂ with epoxides under mild conditions. *Microporous Mesoporous Mater.* **2019**, *274*, 363–372.

(38) Zhu, J.; Usov, P. M.; Xu, W.; Celis-Salazar, P. J.; Lin, S.; Kessinger, M. C.; Landaverde-Alvarado, C.; Cai, M.; May, A. M.; Slebodnick, C.; et al. A New Class of Metal-Cyclam-Based Zirconium Metal–Organic Frameworks for CO₂ Adsorption and Chemical Fixation. *J. Am. Chem. Soc.* **2018**, *140*, 993–1003.

(39) Demir, S.; Usta, S.; Tamar, H.; Ulusoy, M. Solvent free utilization and selective coupling of epichlorohydrin with carbon dioxide over zirconium metal-organic frameworks. *Microporous Mesoporous Mater.* **2017**, *244*, 251–257.

(40) Zhu, J.; Liu, J.; Machain, Y.; Bonnett, B.; Lin, S.; Cai, M.; Kessinger, M. C.; Usov, P. M.; Xu, W.; Senanayake, S. D.; et al. Insights into CO₂ adsorption and chemical fixation properties of VPI-100 metal–organic frameworks. *J. Mater. Chem. A* **2018**, *6*, 22195–22203.

(41) Babu, R.; Kathalikkattil, A. C.; Roshan, R.; Tharun, J.; Kim, D.-W.; Park, D.-W. Dual-porous metal organic framework for room temperature CO₂ fixation via cyclic carbonate synthesis. *Green Chem.* **2016**, *18*, 232–242.

(42) Liu, L.; Wang, S.-M.; Han, Z.-B.; Ding, M.; Yuan, D.-Q.; Jiang, H.-L. Exceptionally Robust In-Based Metal–Organic Framework for Highly Efficient Carbon Dioxide Capture and Conversion. *Inorg. Chem.* **2016**, *55*, 3558–3565.

(43) Dau, P. V.; Kim, M.; Garibay, S. J.; Münch, F. H. L.; Moore, C. E.; Cohen, S. M. Single-Atom Ligand Changes Affect Breathing in an Extended Metal–Organic Framework. *Inorg. Chem.* **2012**, *51*, 5671–5676.

(44) Bloch, E. D.; Britt, D.; Lee, C.; Doonan, C. J.; Uribe-Romo, F. J.; Furukawa, H.; Long, J. R.; Yaghi, O. M. Metal insertion in a microporous metal–organic framework lined with 2, 2'-bipyridine. *J. Am. Chem. Soc.* **2010**, *132*, 14382–14384.

(45) Rao, X.; Cai, J.; Yu, J.; He, Y.; Wu, C.; Zhou, W.; Yildirim, T.; Chen, B.; Qian, G. A microporous metal–organic framework with both open metal and Lewis basic pyridyl sites for high C₂H₂ and CH₄ storage at room temperature. *Chem. Commun.* **2013**, *49*, 6719–6721.

(46) Beyzavi, M. H.; Klet, R. C.; Tussupbayev, S.; Borycz, J.; Vermeulen, N. A.; Cramer, C. J.; Stoddart, J. F.; Hupp, J. T.; Farha, O. K. A hafnium-based metal–organic framework as an efficient and multifunctional catalyst for facile CO₂ fixation and regioselective and enantioselective epoxide activation. *J. Am. Chem. Soc.* **2014**, *136*, 15861–15864.

(47) Carey, F. A.; Sundberg, R. J. *Advanced Organic Chemistry: Part A: Structure and Mechanisms*, Chapter 1; Springer Science & Business Media, 2007; pp 18–22.

(48) Cavka, J. H.; Jakobsen, S.; Olsbye, U.; Guillou, N.; Lamberti, C.; Bordiga, S.; Lillerud, K. P. A new zirconium inorganic building brick forming metal organic frameworks with exceptional stability. *J. Am. Chem. Soc.* **2008**, *130*, 13850–13851.

(49) Gonzalez, M. I.; Bloch, E. D.; Mason, J. A.; Teat, S. J.; Long, J. R. Single-Crystal-to-Single-Crystal Metalation of a Metal–Organic Framework: A Route toward Structurally Well-Defined Catalysts. *Inorg. Chem.* **2015**, *54*, 2995–3005.